

Aerosol Size Distribution



Claudia Di Biagio

Contents

1 Preamble and Definitions.....	202
2 Observations.....	205
3 Synthesis of Observations.....	214
4 Summary and Challenges for Future Research.....	218
References.....	219

Abstract Particle size is a fundamental parameter to understand and predict the lifetime, transport processes, and the diverse impacts of atmospheric aerosols. In this chapter, we review current knowledge on the size distribution of atmospheric aerosols observed in the Mediterranean basin. This includes remote sensing observations, as well as ground-based and airborne in situ measurements from intensive field campaigns over the last two decades. Observations show that the volume aerosol size distribution above 100 nm diameter is basically bimodal in the whole Mediterranean basin, with anthropogenic particles mostly contributing to the fine mode and dust, smoke, and marine particles contributing to the coarse mode. Coarse and giant dust particles measured for Saharan outbreaks agree with similar observations in the Atlantic, supporting the efficient transport of dust aerosols with diameters above 10 μ m over long distances. Ultrafine particles (<100 nm diameter) are ubiquitous over the basin and observed both in the boundary layer and the free troposphere. While past observations provide significant knowledge, at present we still miss a complete regional characterization of the aerosol size over the whole basin

Chapter reviewed by **Konrad Kandler** (Institut für Angewandte Geowissenschaften, Technische Universität Darmstadt, Darmstadt, Germany) and **Marc Mallet** (Centre National de Recherches Météorologiques, Toulouse, France), as part of the book *Part VII Mediterranean Aerosol Properties* also reviewed by **Jorge Pey Betrán** (ARAID-Instituto Pirenaico de Ecología, CSIC, Zaragoza, Spain)

C. Di Biagio (✉)

Université Paris Cité and Univ. Paris Est Créteil, CNRS, LISA, F-75013 Paris, France
e-mail: claudia.dibiagio@lisa.ipsl.fr

including seasonal effects. Further observation and retrieval capabilities from satellites need to be developed to fulfill this gap.

1 Preamble and Definitions

We define in this section the basic information concerning the atmospheric aerosol size distribution, and we introduce the parameters presented and discussed in the chapter. For a complete discussion and analysis of theoretical bases, we redirect the reader to Seinfeld and Pandis (2016).

Atmospheric aerosols cover a vast size spectrum, from few nanometers to tens of micrometers. Particles with diameters less than $1\mu\text{m}$ are classified as “fine aerosols,” while particles greater than $1\mu\text{m}$ are “coarse aerosols.” Fine aerosols are additionally divided into Aitken or ultrafine mode particles (diameter $< 0.1\mu\text{m}$) and accumulation mode particles (diameter between 0.1 and $1.0\mu\text{m}$; to note that in some literature studies the separation between Aitken and accumulation modes is at radius of $0.1\mu\text{m}$ instead of the diameter). The size distribution and the partitioning between the fine and coarse modes for different aerosol types depend first on their formation mechanism. Coarse mode aerosols are usually made of primary particles, mostly of natural origin. Primary aerosol particles are defined as particles directly entrained into the atmosphere by the drag of wind on continental and oceanic surfaces (desert dust or sea salt aerosols), as a product of biomass burning (soot and ashes), volcanic eruptions, or biological debris, among others. In contrast, anthropogenic aerosols occur mostly in the fine mode, and they are often secondary in origin. Secondary aerosols are formed in the atmosphere from gaseous precursors (e.g., new particle formation (NPF) from gas-to-particle conversion), and they can be both natural and anthropogenic. Once in the atmosphere, the aerosol size distribution continuously modifies due to processes like coagulation, sedimentation, heterogeneous reactions with gases, water adsorption, and mixing (Seinfeld & Pandis, 2016).

The size distribution of the aerosols is typically expressed as the number distribution $dN(D)/d\log D$ where $dN(D)$ is the number concentration of particles, i.e., the number of particles per cm^3 of air, per size interval expressed in logarithmic scale ($d\log D = \log(D_2/D_1)$, with D_1 and D_2 the lower and upper diameters of the size bin). Similarly, the number distribution can be expressed as a function of the particle radius (R) as $dN(R)/d\log R$ knowing that the two definitions are equivalent since $d\log D = d\log R$. Both the decimal ($d\log_{10} D$) and the natural ($d\ln D$) logarithm can be used in the size formulation, and both are currently found in the literature. The decimal and logarithmic formulations are related by a constant proportionality that is $dN/d\log D = \ln(10) dN/d\ln D$.

Because several aerosol properties depend on the aerosol surface, volume, and mass, it is often convenient to express the aerosol size distribution in the form of surface size distribution ($dS/d\log D = \pi D^2 dN/d\log D$ in the approximation of spherical particles, unit of $\mu\text{m}^2 \text{cm}^{-3}$), volume distribution ($dV/d\log D = \pi/6 D^3 dN/d\log D$, unit of $\mu\text{m}^3 \text{cm}^{-3}$), and mass distribution ($dM/d\log D = \rho dV/d\log D$, units of

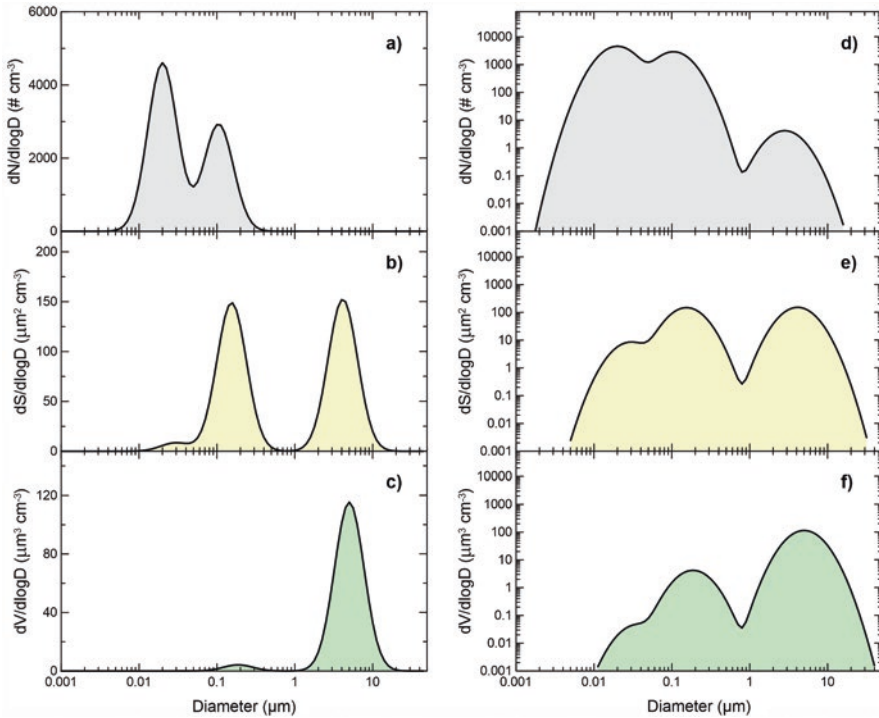


Fig. 1 Example of an atmospheric aerosol size distribution composed of three lognormal modes; **a and d** number size distribution; **b and e** surface size distribution; **c and f** volume size distribution. Distributions are plotted in linear and logarithmic ordinate scales (left and right plots, respectively). (Modified from Fig. 8.6 in Seinfeld and Pandis (2016))

$\mu\text{g cm}^{-3}$, where ρ is the aerosol particle density, e.g., as g cm^{-3}). These formulations represent the distribution of the surface area, volume, and mass of particles per cm^3 of air.

The size distribution of atmospheric aerosols usually appears as the sum of main modes, each of them well represented by a lognormal distribution, i.e., the $\log D$ or $\ln D$ are normally distributed. In Fig. 1, we report an example of number, surface, and volume distribution for a typical atmospheric aerosol population composed of the sum of three lognormal modes including both submicronic and supermicronic particles. The number modal diameter, which is the diameter at which the derivative of the distribution is zero (in other words the mode maximum), is 0.02, 0.10, and $2.8\mu\text{m}$ for the three modes. Figure 1 shows that the submicronic aerosol modes dominate the number distribution (Fig. 1a and d), whereas the supermicronic aerosol mode dominates the volume size (Fig. 1c and f). This is because the volume of a particle of 1 or $10\mu\text{m}$ in diameter is 10^3 or 10^6 times larger than that of a particle of 100 nm in diameter. Showing the size distribution data as a function of number or volume can permit therefore to better evidence the contribution of fine or ultrafine particles (number representation) or coarse mode diameters (volume representation) to the whole dust size spectrum.

The number-, surface-, volume-, and mass-median diameter (NMD, SMD, VMD, and MMD, units of length) are respectively the diameters for which half of the number, surface, volume, and mass of the aerosol population is for diameters below the median diameter and the other half above. For lognormal distributed aerosols, the median diameter coincides with the modal diameter of the distribution. The different median diameters represent different properties of the size distribution, and their values are not directly comparable, with the only exception for the VMD and the MMD that coincide if the aerosol density is constant with size. As an example, for the three modes in Fig. 1, the NMD is 0.02, 0.10, and 2.8 μm , and the VMD is 0.04, 0.2, and 5 μm . The aerosol particle size distribution is generally represented by a sum of lognormal modes, with the advantage that a lognormal size distribution has the same geometric standard deviation (σ) in number, size, or volume and that a simple relationship relates the various median numbers (e.g., $\text{VMD} = \text{NMD} \exp\{3(\ln\sigma)^2\}$; Jaenicke, 1988).

Other size-related parameters frequently used to describe the aerosol size distribution are the (optical) effective radius (R_{eff} ; or the effective diameter D_{eff} , that is twice R_{eff}), the effective variance (v_{eff}), and the Angström exponent of scattering/extinction (α). These are defined as follows.

• **The effective radius (R_{eff}), effective diameter (D_{eff}), and effective variance (v_{eff})**

The effective radius R_{eff} (unit of length), or area-weighted mean radius, is calculated by weighting each radius by the cross-sectional area of the particles ($\pi R^2 dN(R) / d\log R$):

$$R_{\text{eff}} = \frac{\int R\pi R^2 \frac{dN}{d\log R} d\log R}{\int \pi R^2 \frac{dN}{d\log R} d\log R} = \frac{\int \pi R^3 \frac{dN}{d\log R} d\log R}{\int \pi R^2 \frac{dN}{d\log R} d\log R} \quad (1)$$

The corresponding definition of D_{eff} is:

$$D_{\text{eff}} = \frac{\int \pi D^3 \frac{dN}{d\log D} d\log D}{\int \pi D^2 \frac{dN}{d\log D} d\log D} \quad (2)$$

In parallel, we can also define the effective variance, that is, a measure of the width of the aerosol distribution (unitless), as:

$$v_{\text{eff}} = \frac{\int (R - R_{\text{eff}})^2 R^2 \frac{dN}{d\log R} d\log R}{R_{\text{eff}}^2 \int R^2 \frac{dN}{d\log R} d\log R} \quad (3)$$

The term “effective” refers to the light extinction properties of the aerosol population, since the capacity of aerosols to extinct radiation is proportional to the cross-sectional area in the limit of geometric optics, i.e., when the radius of the particle is similar or larger than the wavelength of the incident light. Therefore, the effective radius or effective diameter are particularly useful when referring to the optical properties of aerosols. Aerosol populations with both the same R_{eff} (or D_{eff}) and ν_{eff} will show a similar optical behavior. The R_{eff} or D_{eff} can be calculated for the entire aerosol size distribution (entire range of documented radius or diameters) or evaluated separately for the fine and coarse fractions of the aerosols size, for instance, by integrating Eq. 2 for diameters $\leq 1\mu\text{m}$ ($D_{\text{eff, fine}}$) and $>1\mu\text{m}$ ($D_{\text{eff, coarse}}$), respectively. It should be mentioned that the retrieved values for the fine and coarse effective radius or diameter critically depend on the selected size range of calculation, i.e., the lower and upper limit of the documented size distribution. As a consequence, the R_{eff} and D_{eff} from sizes measured with instruments with different dynamical ranges are not always directly comparable.

- **The Angström Exponent (AE)**

The unitless Angström exponent (AE) represents the spectral dependence of extinction or aerosol optical depth (AOD). The AOD depends on the wavelength (λ) of light according to the power law (Angström, 1929):

$$AOD_{\lambda} = AOD_{\lambda_0} \left(\frac{\lambda}{\lambda_0} \right)^{-AE} \quad (4)$$

The Angström exponent is the exponent of the power law in Eq. 4. For non-absorbing aerosols, the Angström exponent is a good proxy for the aerosol particle size distribution: in general, the larger the particles, the lower AE, and vice versa.

2 Observations

Currently, most of the knowledge on the Mediterranean aerosol size distribution is derived from in situ and remote sensing measurements. The majority were made at coastal sites around the basin or at island locations. Also, local- and regional-scale intensive studies including aircraft and balloon-borne observations importantly contributed.

2.1 Ground-Based Remote Sensing Measurements

The AERONET (Aerosol Robotic Network; <https://aeronet.gsfc.nasa.gov>), due to its extensive coverage of the area and the long-term track of observations available (more than 20 years for some stations), is the first source of information on the size

distribution for Mediterranean aerosols. The AERONET network is a global network of ground-based multi-spectral sun and sky photometers measuring daytime aerosol load and properties (Holben et al., 1998). The AERONET operational analysis protocol retrieves the aerosol size distribution in the range 0.1–30 μm in diameter by mathematical inversion of combined direct solar irradiance and sky radiance measurements (Dubovik & King, 2000; Dubovik et al., 2006). In this case, the retrieved size distribution is column-integrated, that is, it represents the mean size distribution of the various aerosol layers encountered from ground level up to the top of the atmosphere. The AERONET retrievals, being based on remote sensing measurements of the aerosol optical signature, depend on particle shape (Dubovik et al., 2006). The latest AERONET retrieval scheme works considering an aerosol mixture of polydisperse randomly oriented homogeneous spheroids with a fixed distribution of aspect ratios (Mishchenko et al., 1997; Dubovik et al., 2006).

As of mid-2022, there are about 50 active AERONET sites around the Mediterranean basin (see Fig. A1 in the volume annex; Dulac et al., 2023). Their regional distribution is quite homogeneous and covers the western and the eastern parts, from southern Europe to the coasts of Middle East and North Africa, including also many island locations throughout the area (Ersa, Palma de Mallorca, Lampedusa, Alboran, Malta, Crete, etc.). This spatial extent allows for capturing the diversity of the Mediterranean aerosol population resulting from the different contributing sources, such as desert dust, marine, urban/industrial pollution, and biomass burning, showing particles in the 0.1–30 μm optically active range sensed by AERONET. On the other hand, AERONET observations do not provide information on the aerosol ultrafine mode, therefore no indications of NPF events.

Various studies reporting AERONET observations across the Mediterranean discuss the retrieved column-integrated volume distributions (e.g., Kubilay et al., 2003; Masmoudi et al., 2003a, b; Derimian et al., 2006; Toledano et al., 2007; Mallet et al., 2013, 2016; Sicard et al., 2016; Logothetis et al., 2020) or the Angström exponent (e.g., Sabbah et al., 2001; Pace et al., 2006; Basart et al., 2009; Formenti et al., 2018; Logothetis et al., 2020). A statistical study of the long-term AERONET size data across the Mediterranean basin was performed by Mallet et al. (2013) using datasets from 22 AERONET coastal stations with more than 2.5 yr of data. They showed that the volume size distribution of the aerosols in the basin is bimodal and that the coarse mode usually dominates over the fine mode (Fig. 2): in the eastern (western) part of the Mediterranean, they found a 31% (37%) average contribution from the fine mode and 69% (63%) contribution from the coarse mode to the total particle's volume size. The average modal diameter for the fine mode is located around 0.3 μm , whereas for the coarse mode, it is between 4.5 and 5.0 μm (Mallet et al., 2013, 2016). Daily and seasonal data show nonetheless a spread of both modal diameters and concentration values for the fine and coarse modes due to the variable contribution of different aerosol types and loading conditions (Mallet et al., 2016; Sicard et al., 2016).

Gkikas et al. (2016) made a similar statistical study than Mallet et al. (2013), but also included inland areas around the basin for a total of 109 stations from the year 2000 to 2013. They found that the two distinct fine and coarse modes in the

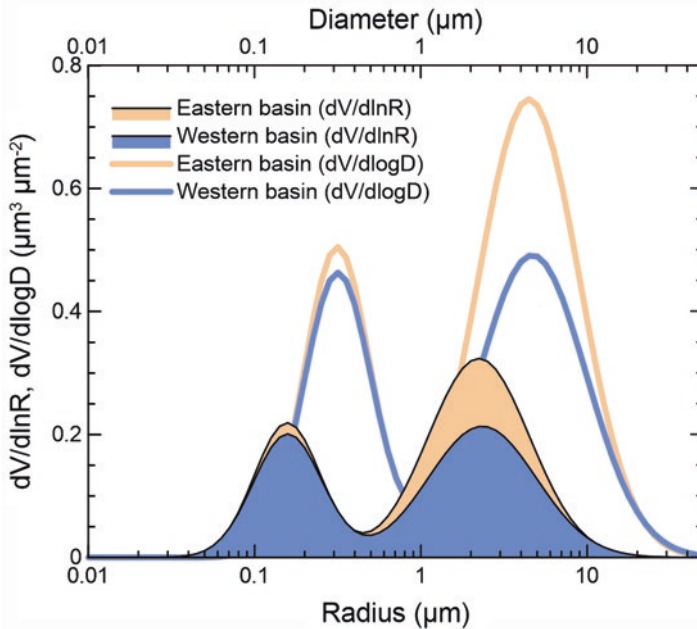


Fig. 2 Average volume size distribution retrieved from AERONET inversions at 8 coastal sites in the eastern Mediterranean basin and 14 coastal sites in the western basin. We show here both the $dV/d\ln R$ distributions as provided by Mallet et al. (2013) and given as AERONET output and also the conversion into $dV/d\log D$ formulation. Note that the unit for the volume distribution is $\mu\text{m}^3 \mu\text{m}^{-2}$ in AERONET as it refers to a column-averaged quantity. (Modified from Fig. 8 in Mallet et al. (2013))

climatological aerosol size distribution (average modal diameters at 0.3 and $4.4\mu\text{m}$) equally contribute to the volume size, differently from Mallet et al. (2013), where this difference was due to the larger contribution of finer aerosols from continental Europe included in their study. They also analyzed the shape of the distribution under strong and severe dust episodes and found in these cases that the size is still bimodal (about 0.3 and 3.4 – $4.5\mu\text{m}$ modal diameters for the fine and coarse modes), but the peak of the coarse mode increases by up to 15 times due to the contribution of coarse dust, in accordance with other studies (e.g., Kubilay et al., 2003; Tafuro et al., 2006). Also for fresh smoke plumes measured in coastal Spain, the size is bimodal. The fine mode is centered at 0.26 – $0.29\mu\text{m}$ (volume modal diameter), similarly to dust, and the coarse mode is at about $5.0\mu\text{m}$ (Alados-Arboledas et al., 2011; Gómez-Amo et al., 2017). This agrees with AERONET values reported for biomass burning aerosols all over the world (Sayer et al., 2014). Similar to dust and smoke, marine aerosols observations at the Ersa site in northern Corsica in summer 2013 show a fine mode located around $0.3\mu\text{m}$, but a larger coarse mode at about $7\mu\text{m}$, consistently with in situ surface data taken at the same site (Claeys et al., 2017). The study by Gerasopoulos et al. (2007) compared the mass size distributions obtained by cascade impactor sampling to those retrieved by AERONET between

2004 and 2006 at a remote coastal station in Greece. Seven distinct modes are identified in the diameter range 0–10 μm . Of these, the “Accumulation 1” (0.25–0.55 μm) and “Coarse 2” (3–7 μm) modes are dominant, in line with the AERONET studies.

2.2 *In Situ Measurements*

In order to more thoroughly characterize the impacts of atmospheric aerosols on climate and health, one has to know their number, surface, and volume/mass size distributions on the largest possible size spectrum, including ultrafine and coarse diameters. This type of measurement is complex, as it requires a combination of various in situ analyzers based on different physical principles for different size classes. The submicron fraction of atmospheric aerosols is commonly sized in terms of the electrical mobility diameter (i.e., the diameter of a sphere with the same migration velocity in a constant electric field as the particle of interest) by using the differential mobility particle sizer (DMPS), working in the range going from few nm up to 900 nm. Optical particle counters (OPCs) use the light scattering technique to provide the aerosol number size distribution between approximately 300 nm to 100 μm as optical equivalent diameter (i.e., the diameter of a sphere of given or assumed refractive index scattering the same amount of radiation into a given solid angle). Aerosol sizing over a large diameter range including supermicron diameters can be also performed by individual particle characterization by transmission and/or scanning electron microscopy on particles collected by filtration or impaction; in this case, the size distribution is expressed as a function of the projected–area equivalent diameter (i.e., the diameter of a circle with the same area of the particle under investigation as obtained from the 2-dimensional aerosol image projection). The aerosol size distribution in terms of the aerodynamic diameter (i.e., the diameter of a sphere of unit density having the same terminal velocity in an accelerated airflow as the irregularly shaped particles) can be measured by Aerodynamic Particle Sizers (APS), working in the range going from about 500 nm to 20 μm . Finally, multistage filtration or cascade impaction sampling coupled with gravimetric or chemical analysis can be applied to retrieve the mass size distributions of aerosols. The full aerosol number/mass size distribution over the entire sub- to supermicron diameter range can be reconstructed from the combination of these different measurement techniques, an exercise which however is far from being without ambiguity (e.g., DeCarlo et al., 2004; Formenti et al., 2011; Ryder et al., 2013) for two main reasons: first, the necessity to refer to a same diameter definition (electrical mobility, optical, projected-area, aerodynamic) when combining different datasets, which implies performing a priori assumptions on the physicochemical properties of the (generally unknown) aerosol population and, second, the possible occurrence of size-dependent biases possibly varying with the sizing technique as a function of the specific sampling conditions, i.e., lowered sampling efficiencies for specific size ranges. This second issue may particularly affect airborne data from research aircraft

due to the low pressure and high speed (Ryder et al., 2013). In order to ensure the robustness of the obtained aerosol size distribution, whenever it is possible, the accuracy of the collected data should be evaluated through validation/intercomparison studies based on mass and optical closures.

Numerous intensive campaigns using both ground-based, airborne, and balloon-borne platforms reported on in situ measurements of the number and mass size distributions across the Mediterranean basin using mostly optical and condensation counters and multistage impactor sampling (Table 1). Although spatially sparse and often focused on specific events, these data constitute the most accurate method for describing in detail the spatial and vertical variability of the aerosol size distribution on scales ranging from local to regional. In particular, airborne observations are among the only in situ data of aerosol size distribution over the sea surface. Often the mass size distribution is reported for individual chemical components by using a combination of impactor sampling and analysis by ion beam or chemical extraction techniques (e.g., Dulac et al., 1989; Ichoku et al., 1999; Maenhaut et al., 1999; Formenti et al., 2001; Masmoudi et al., 2003b; Smolík et al., 2003; Kuloglu & Tuncel, 2005). This allows distinguishing the relative contribution of anthropogenic and natural sources to the aerosol load. As an example, at Sde Boker in Israel, the fine mode mass distribution is dominated by anthropogenic aerosols generated by conversion of long-range transported SO₂ and other combustion products, whereas an enhancement in the coarse mode is related to intrusion of Saharan mineral dust (Maenhaut et al., 1999). These authors were also able to identify the seasonal cycle in the relative contributions of pollution and dust to size distribution.

Recent airborne data, and in particular those acquired during the project ChArMEx (Chemistry-Aerosol Mediterranean Experiment) including the TRAQA, SAFMED, and ADRIMED surface and airborne campaigns in summers 2012 and 2013, have provided new data of the ultrafine and coarsest aerosol modes and their vertical and spatial distribution across the Mediterranean, which we explore further in the two following paragraphs.

2.3 In Situ Observations of the Ultrafine Particle Mode

As part of ChArMEx, the TRAQA and SAFMED airborne campaigns in the north-western Mediterranean basin have evidenced the presence of both fine and ultrafine aerosols as far as 250 km from the coastline (and up to 4 km in height) in summertime (Di Biagio et al., 2015, 2016). The combined analysis of the plumes chemical composition and size suggested the mixing of fresh and aged pollution air masses mostly corresponding to export from inland areas and coastal cities in southern Europe. Below 350 m in the boundary layer, the volume size distribution had two equally abundant main modes, occurring frequently in the Mediterranean as indicated from AERONET observations. The fine mode is centered between 0.13 and 0.23 μm and the coarse one between 5 and 8 μm as number modal diameter (NMD), corresponding to a fine mode of 0.15–0.25 μm and a coarse mode between 4 and

Table 1 Summary of intensive studies targeted at aerosol physicochemical and radiative properties and including size observations performed in the Mediterranean basin in the last two decades based on in situ measurements using ground-based and airborne platforms

Location	Level/ Platform	Campaign	Period	References
Negev desert, Israel	Surface	ARACHNE (Aerosol, RAAdiation and CHEmistry Experiment)	Summer 1996	Ichoku et al. (1999) Maenhaut et al. (1999), Formenti et al. (2001), Andreae et al. (2002)
Thessaloniki, Greece	Surface	MEDUSE (Mediterranean DUST Experiment)	June 1997	Chazette and Liousse (2001)
Southern Aegean Sea and Finokalia, Crete	Airborne and surface	STAAARTE (Scientific Training and Access to Aircraft for Atmospheric Research Throughout Europe)	June 1997	Dulac and Chazette (2003)
Aegean Sea	Airborne	STAAARTE-MED (Scientific Training and Access to Aircraft for Atmospheric Research Throughout Europe - Mediterranean campaign)	Summer 1998	Formenti et al. (2002)
Lampedusa Isl., Italy	Airborne, Surface	PAUR (Photochemical Activity and Ultraviolet Radiation)	May 1999	Junkermann (2001), Di Iorio et al. (2003)
Mt. Cimone, Italy	Surface	MINATROC (Mineral Dust and Tropospheric Chemistry)	June–Dec. 2000	Bonasoni et al. (2004)
			June–July 2000	Van Dingenen et al. (2005)
Lampedusa Isl., Italy	Surface	C–MARE (Central Mediterranean Aerosol and Radiation Experiment)	Sept.–Oct. 2004	di Sarra et al. (2005)
	Airborne, Surface	GAMARF (Ground–based and Airborne Measurement of the Aerosol Radiative Forcing)	April–May 2008	Meloni et al. (2015)
Basilicata, Italy	Airborne	MORE (Marine Ozone and Radiation Experiment)	June 2010	Pace et al. (2015)
Southern France	Surface	ESCOMPTE (Expérience sur Site pour Contraindre les Modèles de Pollution atmosphérique et de Transport d’Emissions)	June–July 2001	Mallet et al. (2003)
Barcelona, Spain	Surface	–	Nov. 2003–Dec. 2004	Pey et al. (2008) Pey et al. (2009) Dall’Osto et al. (2012)
	Surface	SAPUSS (Solving Aerosol Problems by Using Synergistic Strategies)	Fall 2010	Brines et al. (2014)

(continued)

Table 1 (continued)

Location	Level/ Platform	Campaign	Period	References
Montseny, Spain	Surface	–	Nov. 2010–May 2011 and mid-Oct. 2011–mid-Dec. 2011	Cusack et al. (2013a, 2013b)
Western Mediterranean	Airborne	HYMEX (HYdrological cycle in Mediterranean Experiment)	Sept.–Nov. 2012	Rose et al. (2015)
	Balloon-borne	ChArMEx (the Chemistry-Aerosol Mediterranean Experiment)	Summer 2013	Renard et al. (2018)
	Airborne	TRAQA (Transport and Air Quality)	June–July 2012	Di Biagio et al. (2015, 2016)
	Airborne	SAFMED (Secondary Aerosol Formation in the MEDiterranean)	July 2013	
	Airborne, Surface	ADRMED (Aerosol Direct Radiative Impact on the regional climate in the MEDiterranean region)	June 2013	Denjean et al. (2016), Mallet et al. (2016)
Lampedusa Isl., Italy	Surface		June 2013	Mallet et al. (2016, 2019)
Ersa (Corsica Isl.), France and Finokalia (Crete Isl.), Greece	Surface	ChArMEx (the Chemistry-Aerosol Mediterranean Experiment) enhanced observation period (EOP)	May 2012–August 2013	Berland et al. (2017)

9.6 μm as VMD. High number concentrations (up to 20,000 cm^{-3}) of ultrafine or Aitken particles, measured in the size range 4–100 nm, were observed in several cases, both in the boundary layer and in the free troposphere during the TRAQA and SAFMED campaigns. Examples of different Aitken and accumulation mode aerosol vertical concentration profiles during TRAQA showing layers with enhanced Aitken mode particles are shown in Fig. 3.

Some of the cases observed during TRAQA and SAFMED corresponded to a concurrent increase in the concentration of accumulation mode particles. As shown for instance in Fig. 3a, which refers to the SAFIRE ATR-42 flight V31, the dN_{Aitken} increase between 1000 and 3000 m corresponds to simultaneous increase of dN_{Acc} (but also CO and ozone not reported in the figure), suggesting a layer directly transported from a region emitting in the Aitken size range. In other cases, the ultrafine aerosol was not related to simultaneous accumulation mode and ozone increases in the layer, suggesting the occurrence of NPF events over the basin. Panel (b) corresponds to flight V28b: the enhanced dN_{Aitken} layer at about 100 m, not related to dN_{Acc} increase, is possibly related to surface emissions over the sea surface (e.g., ship emissions) and NPF events. Panel (c) corresponds to flight V26: the layer

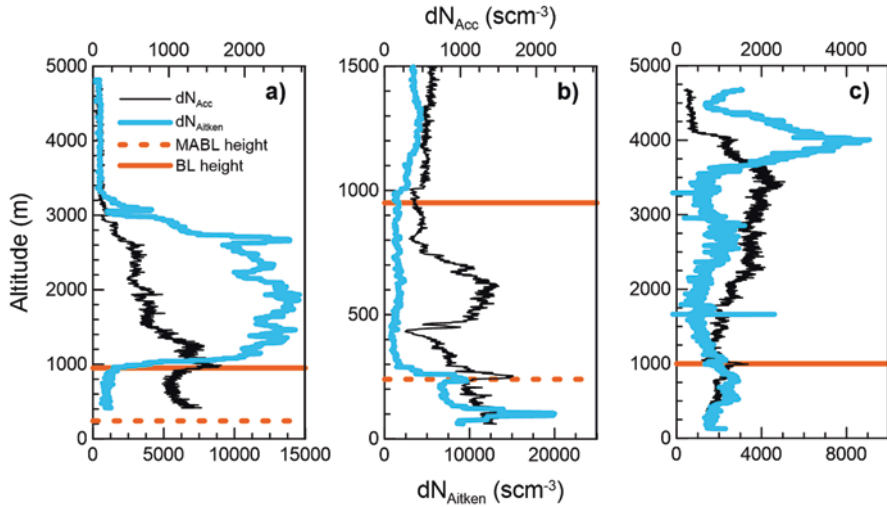


Fig. 3 Vertical profiles of the accumulation and Aitken number particle concentrations (dN_{Acc} , dN_{Aitken}) for three flights of the SAFIRE ATR-42 during the TRAQA campaign. The horizontal lines indicate the height of the marine atmospheric boundary layer (MABL; dotted line) and the planetary boundary layer (BL; continuous line): (a) flight V31; (b) flight V28b; (c) flight V26. Particle concentrations are expressed as the number of particles per standard cubic centimeter (i.e., at standard temperature and pressure (STP) conditions $T = 293.15$ K and $p = 1013.25$ hPa). (Modified from Fig. 10 in Di Biagio et al. (2015))

of enhanced dN_{Aitken} in the free troposphere between 3500 and 4500 m is possibly related to a NPF event.

Measurements of ultrafine particles are rare in the Mediterranean with only few long-term time series of in situ observations available in coastal areas in the western (Pey et al., 2008; Cusack et al., 2013a) and eastern (Kopanakis et al., 2013; Kalivitis et al., 2019) parts of the basin. Additional data are available over the sea surface from past intensive field campaigns. Airborne measurements during the C-MARE and GAMARF campaigns in the open sea site of Lampedusa reported ultrafine particle concentrations lower than 3000 cm^{-3} in the boundary layer (di Sarra et al., 2005; Meloni et al., 2015). Concentrations up to $12,000\text{ cm}^{-3}$ for ultrafine aerosols were obtained at a coastal site with complex orography in Southern Italy during the MORE experiment with evidence of local pollution and possibly nucleation phenomena associated with the events (Pace et al., 2015). The study by Rose et al. (2015) based on HYMEX observations also reported on NPF events over the open sea in the western basin. These authors showed that NPF events occur over large areas above the sea in mass types with different origins. Observations by Rose et al. further indicate that significant high concentrations of particles in the size range 5–10 nm correspond to fetches (time spent by the air mass over the sea surface) spanning between 0 and 60 h and that ultrafine concentration maxima do not consistently correspond to low fetches, therefore supporting the hypothesis that local marine precursors may significantly contribute to NPF over the basin. Mallet

et al. (2005) reported on ultrafine aerosol measurements during a summertime photochemical pollution event in the Marseille area, Southern France, 60 km inland. They measured vertical profiles of particles' concentration larger than 7 nm in two consecutive days in the early morning and at noon. The aerosol concentration in the boundary layer was observed in both days to be lower in the morning (4000 cm^{-3}) than at noon, when it reached values of $12,000 \text{ cm}^{-3}$ in the first day and more than $40,000 \text{ cm}^{-3}$ in the second day of measurements. Berland et al. (2017) reported on ground-based measurements at Ersa (Corsica) and Finokalia (Crete) over a 1-year period (2013) and for the 2013 summer season also at Mallorca (Spain) and combined to aircraft data during ADRIMED and SAFMED to study the contribution of NPF at the scale of the basin. They found that NPF events leading to enhanced ultrafine particle concentrations occurred about 35% of the time at Ersa and Finokalia with a similar seasonal pattern showing a maximum in spring. The NPF formation was interestingly observed for 20% of the cases to occur simultaneously at least at two of the three stations considered, which suggests the regional-scale character of NPF events and ultrafine particle distribution in the Mediterranean area. In another chapter of this book, Junkermann (2022) also reports ultrafine particle size distribution measurements performed with an ultralight aircraft up to 3.5 km in altitude in Corsica and Malta during TRAQA and ADRIMED campaigns, respectively. The role of shipping as a large source of ultrafine particles over the Mediterranean is highlighted.

2.4 In Situ Observations of the Coarse Mineral Dust Particle Mode

Airborne measurements during the ChArMEx campaign in 2013 have also provided new data on the size of Saharan dust under transport conditions with particular focus on its coarsest sizes. First observations of the coarse dust size distribution were provided in few studies over the basin (e.g., De Falco et al., 1996).

An accurate description of the coarse mode of mineral dust is vital since the presence of large particles enhances the capacity of mineral dust in absorbing shortwave and longwave radiation (e.g., Ryder et al., 2013) and affects cloud formation (e.g., Koehler et al., 2009) and atmospheric chemistry (e.g., Bauer et al., 2004). Aircraft observations of dust aerosols above 1.5 km in the western Mediterranean during ADRIMED were reported in Denjean et al. (2016). The dust number size distribution was parameterized as a four-mode lognormal function, and the coarse mode was located between 1.3 and $2.5 \mu\text{m}$ (number modal diameter or NMD, corresponding to values between about 7 and $19 \mu\text{m}$ for the VMD) regardless of the altitude, indicating a vertically well-mixed coarse mode. Below 300 nm in diameter, the dust aerosols were externally mixed with pollution particles. The effective coarse diameter ($D_{\text{eff, coarse}}$, calculated between 1 and $20 \mu\text{m}$) was within 3.8 and $14.2 \mu\text{m}$ independently of the transport time (estimated at 1–5 days for the measured episodes during

ADRMED), suggesting that the dust transported over the Mediterranean conserves its coarse mode. This persistence of the coarse mode was explained in Denjean et al. (2016) by the presence of temperature inversions in the middle troposphere, as observed from aircraft sondes, which kept the dust confined in a stable stratified layer. Additional observations were performed with sounding and quasi-Lagrangian drifting balloons launched from Menorca island in the western Mediterranean and embarking a new OPC counter (Renard et al., 2016, 2018). The balloon OPC measured persistently aerosols larger than $15\mu\text{m}$ in diameter within a dust plume sampled between the 16th and the 19th of June originated a few days before in northern Africa, in agreement with aircraft observations over the same area by Denjean et al. (2016). The size distribution could be fitted by a sum of three lognormal modes centered at (0.26 ± 0.04) , (3.7 ± 0.4) , and $(30.4 \pm 2.8) \mu\text{m}$ as volume median diameter, which remained fairly stable during the transport over the basin. The persistence of unexpected large particles (up to $50\mu\text{m}$ in diameter) as observed in Renard et al. (2018) suggests that a giant mode of dust aerosols is also efficiently transported in the Mediterranean basin, even if the mechanisms for this transport are still unknown since gravitational settling should quickly scavenge such a mode from the transported plume (e.g., Foret et al., 2006; Weinzierl et al., 2011).

Similarly, to the Mediterranean basin, particles larger than $10\mu\text{m}$ are measured after mid-range transport over the Atlantic Ocean (e.g., Ryder et al., 2013, 2018; Weinzierl et al., 2011, 2017), and indications for the long-range transport of giant mode dust also over the Atlantic are provided by van der Does et al. (2018). Figure 4 compares the datasets of dust volume distribution measured in the Mediterranean by Denjean et al. (2016) with observations performed in the outflow of African dust in the eastern tropical Atlantic. Despite some differences in the submicron size fraction, i.e., an enhanced fine mode in the Denjean et al. (2016) dataset due to the mixing of dust aerosols with pollution particles in the Mediterranean, the data comparison in Fig. 4 suggests the consistency of the dust coarse mode conservation after mid- to long-range transport in the atmosphere.

3 Synthesis of Observations

As discussed in the previous paragraphs, a large body of observations of the Mediterranean aerosols size distribution is available thanks to long-term monitoring and intensive field campaigns. Data have been acquired with different techniques measuring number or mass/volume particle size distributions and different size-related diameters (e.g., optically effective, projected cross area, aerodynamic equivalent, etc.), and more or less constrained hypotheses, often different from a study to another, are necessary to convert one distribution to the other. Despite these difficulties, Tables 2 and 3, respectively, present (i) a synthesis of mass median diameters (MMD) given as EAD (equivalent aerodynamic diameter) obtained by cascade impactor sampling at various ground-based locations and for various

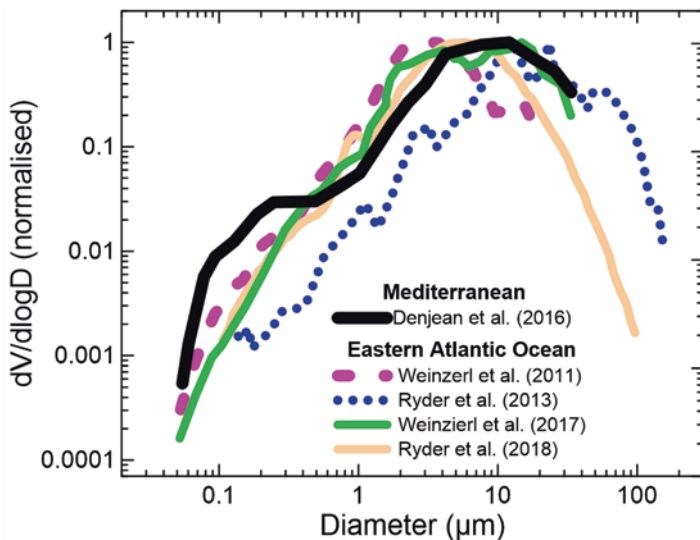


Fig. 4 Volume size distributions of dust aerosols measured airborne during the ADRIMED campaign and comparison to in situ dust size distribution measurements from campaigns in the eastern Atlantic Ocean. Data from Denjean et al. (2016) refer to the average dust size distribution in Fig. 7b; data from Weinzierl et al. (2011) are retrieved from the average number size distribution for dust in their Fig. 13; data from Ryder et al. (2013) refer to the dust “aged” category that is dust emitted 12–70 h prior in the Sahara Desert and are from their Fig. 2; data from Weinzierl et al. (2017) refer to observations at Cape Verde during a Lagrangian experiment and are retrieved from number distribution data in their Fig. 9; data from Ryder et al. (2018) are for the average of dust observations in the Saharan Air Layer (SAL) in their Fig. 6. For the sake of comparison, and in order to eliminate differences linked to different sampled concentrations, all size data are normalized to 1 at the maximum of the volume distribution. (Data are retrieved from cited publications)

aerosol types and (ii) effective diameters D_{eff} obtained by AERONET or sun photometer retrievals across the basin.

In the case of mineral dust, MMD values vary between 2.3 and 6 μm at various sampling sites located in transport regions, the highest values being obtained for the Israeli site of Sde Boker (Formenti et al., 2001; Maenhaut et al., 1999), possibly the closest to North African sources and itself located in a semi-arid environment. The effective diameter values for the coarse mode retrieved by AERONET are in the range 3.2–5 μm for observations conducted in the proximity of source regions in Tunisia (Masmoudi et al., 2003a) and over transport areas in Turkey (Kubilay et al., 2003), Italy (Masmoudi et al., 2003a), and Spain (Gómez-Amo et al., 2017). In agreement with the in situ airborne observations during ChArMEx (Denjean et al., 2016; Renard et al., 2018), these observations suggest that changes in the coarse mode size distribution of dust aerosols due to transport are not important (or detectable) within the precision of optical and aerodynamic measurements.

From these studies, it is also indicated that, apart from dust, there are other contributors to the aerosol coarse mode. Among the non-dust types, the largest coarse

Table 2 Mass median diameter (MMD) as equivalent aerodynamic diameter obtained by impactor sampling and elemental analysis at various ground-based locations and for various aerosol types

Aerosol type	Location	Tracer	MMD (μm)	References
Sea salt	Western Mediterranean Sea	Na	4.6–10.8, median 5.9	Dulac et al. (1989)
	Antalya, Southern Turkey	Cl	5.3	Kuloglu and Tuncel (2005)
	Finokalia, Crete, and Aegean Sea		5	Smolík et al. (2003)
Mineral dust	Capo Cavallo, Corsica	Al	2.3 \pm 0.4	Dulac et al. (1989)
	Western Mediterranean Sea		1.9–5.2, median 2.8	
	Sde Boker, Negev Desert, Israel		6	Maenhaut et al. (1999) Formenti et al. (2001)
	Finokalia, Crete, and Aegean Sea		4	Smolík et al. (2003)
	Antalya, Southern Turkey		3.45	Kuloglu and Tuncel (2005)
Anthropogenic pollution	Sde Boker, Negev Desert, Israel	V	0.3 and 6	Maenhaut et al. (1999) Formenti et al. (2001)
	Finokalia, Crete, and Aegean Sea		0.3 and 3	Smolík et al. (2003)
	Antalya, Southern Turkey		1.21	Kuloglu and Tuncel (2005)
	Western Mediterranean Sea	Pb	0.69	Dulac et al. (1989)
	Finokalia, Crete, and Aegean Sea		1	Smolík et al. (2003)
	Antalya, Southern Turkey		0.77	Kuloglu and Tuncel (2005)
	Finokalia, Crete, and Aegean Sea	S	0.3 and 3	Smolík et al. (2003)
	Antalya, Southern Turkey		0.63 ^a	Kuloglu and Tuncel (2005)
	Zn	1.24	(2005)	

^aAs SO₄²⁻

effective diameters are observed during extremely intense biomass burning events (> 4.0 μm in Gómez-Amo et al. (2017) for a biomass burning smoke event with an exceptional AOD of 8 at 500 nm wavelength as estimated from AERONET observations). These intense fires can lift large carbon aggregates, ashes, and unburnt material quite efficiently.

Another important finding of recent studies is that the aerosol number and mass concentration – in particular for the fine mode – measured in remote regions over the sea surface across the basin are comparable to that measured in coastal cities and

Table 3 Overview of mean effective diameter (D_{eff}) of column-integrated volume distributions of aerosols retrieved over the Mediterranean basin by AERONET or other sun photometer observations. Fine, coarse, and total indicate that data refer to the fine mode, coarse mode, and total size distribution, respectively. Data for Kubilay et al. (2003) and Gómez-Amo et al. (2017) for fine and coarse effective diameters have been recalculated from the published size distribution by applying Eq. (2) and by assuming that the separation between fine and coarse particles occurs for a radius (diameter) of 0.5 (1) μm . Note that the same criteria is not applied in all datasets: Logothetis et al. (2020) assume fine and coarse particles for radius respectively below and above 0.992 μm in their calculations

Location	Dominant aerosol type	D_{eff} (μm)	References
Erdemli, South coastal Turkey (36°N, 34°E), 3 m a.s.l.	Desert dust	0.12 (fine) 3.9 (coarse)	Kubilay et al. (2003)
Thala, Tunisia (35°N, 8°E), 1091 m a.s.l.	Average over April–June 2001	4.6 \pm 0.84 (coarse)	Masmoudi et al. (2003a)
Oristano, Sardinia Isl., Italy (39°N, 8°E), 10 m a.s.l.		4.7 \pm 0.60 (coarse)	
Rome Tor Vergata, Italy (41°N, 12°E), 130 m a.s.l.		5.0 \pm 0.58 (coarse)	
Crete Isl., Greece (35.3°N, 25.3°E), 20 m a.s.l.	Average over Jan. 2003–Dec. 2004	0.26 (fine) 4.2 (coarse)	Fotiadi et al. (2006)
Granada, Spain (37°N, 4°W), 680 m a.s.l.	Biomass burning	0.3–0.4 (total)	Alados-Arboledas et al. (2011)
109 stations within 29–47°N, 11°W–39°E	Aerosol climatology 2000–2013	0.7 (total, median)	Gkikas et al. (2016)
	Desert dust climatology 2000–2013	1.1–2.8 (total) 1.5 (total, median)	
Valencia, Spain (40°N, 0.4°W), 60 m a.s.l.	Summer background	0.22 (fine) 4.1 (coarse) 0.6 (total)	Gómez-Amo et al. (2017)
	Desert dust	0.25–0.36 (fine) 3.2–3.8 (coarse) 1.0–1.6 (total)	
	Smoke	0.25–0.27 (fine) 4.0–4.3 (coarse) 0.4–0.7 (total)	
	Residual smoke	0.22 (fine) 4.1–4.4 (coarse) 0.7–0.8 (total)	
South Europe (9 stations)	Aerosol climatology 2008–2017	0.28–0.38 (fine) 3.86–4.92 (coarse) 0.6–1.0 (total)	Logothetis et al. (2020)
North Africa and the Middle East (10 coastal stations)		0.22–0.30 (fine) 3.46–3.80 (coarse) 1.00–1.42 (total)	

Table 4 Comparison of the number concentrations (in number per standard cm^{-3}) in the Aitken (dN_{Aitken} , 4–100 nm) and accumulation (dN_{Acc} , 0.1– $1\mu\text{m}$) modes observed during the two ChArMEx/TRAQA and ChArMEx/SAFMED airborne field campaigns, together with those reported in the literature for airborne observations in continental Europe

Atmospheric layer	Particle mode	Particle number concentration (scm^{-3})	
		TRAQA and SAFMED campaigns	Other literature over continental Europe
Free troposphere	dN_{Aitken}	0–19250	812–9149 ^a ; 0–980 ^b
	dN_{Acc}	34–3233	20–80 ^c ; 25–85 ^b ; 0–500 ^d
Boundary layer	dN_{Aitken}	4–22471	1037–31370 ^a ; 1000–20000 ^c ; 0–30000 ^f ; 0–19000 ^b
	dN_{Acc}	90–3215	70–560 ^c ; 10–50 ^e ; 400–1200 ^b ; 0–2000 ^d

Adapted from Table 2 in Di Biagio et al. (2015)

^aMallet et al. (2005), south-eastern France, June 2001; size range dN_{Aitken} (0.006– $0.6\mu\text{m}$)

^bHamburger et al. (2012), central Europe, May 2008; size range dN_{Aitken} (0.004– $0.15\mu\text{m}$), dN_{Acc} ($>0.15\mu\text{m}$)

^cPetzold et al. (2002), central Europe, July–August 1998; size range dN_{Acc} ($>0.15\mu\text{m}$)

^dHighwood et al. (2012), central Europe, May 2008; size range dN_{Aitken} (0.004– $0.15\mu\text{m}$), dN_{Acc} ($>0.15\mu\text{m}$)

^eWiegner et al. (2006), Germany, May 2003; size range dN_{Aitken} ($>0.01\mu\text{m}$), dN_{Acc} ($>0.3\mu\text{m}$)

^fJunkermann (2009), Po Valley, July–August 2002 and September–October 2003; size range dN_{Aitken} ($>0.01\mu\text{m}$)

continental Europe, suggesting that a non-polluted atmosphere over the Mediterranean is very rare. This point is illustrated in Table 4 where the number concentrations for Aitken and accumulation mode particles measured over the sea in the Western Mediterranean basin in Di Biagio et al. (2015) are compared to literature values for continental Europe. On the contrary, in clear conditions, as often observed in case of high wind speeds (Mallet et al., 2019), the ultrafine particles concentration over the basin can be lower than 500 cm^{-3} and the accumulation mode concentration lower than 20 cm^{-3} (Pace et al., 2015; Di Biagio et al., 2015). For comparison, the number concentration for the coarse mode ($>1\mu\text{m}$ diameter) may reach 4–40 cm^{-3} for moderate to intense dust events (Bonasoni et al., 2004; Di Biagio et al., 2015; Pace et al., 2015; Denjean et al., 2016).

4 Summary and Challenges for Future Research

The ensemble of observations discussed in this section points out different aspects of the size distribution for Mediterranean aerosols: (i) in the Mediterranean basin, the volume size distribution above 100 nm in diameter is basically bimodal, with anthropogenic particles mostly contributing to the fine mode, while different particle types contributing to the coarse mode (dust, smoke, marine particles); (ii) ultrafine particles ($<100\text{ nm}$ diameter) are ubiquitous over the basin, and NPF events mostly leading to these ultrafine particles occur at the regional scale over the basin,

independently of the air mass origin, and both in the boundary layer and the free troposphere; (iii) observations of coarse and giant particles during dust events are in agreement with similar observations in the Atlantic and support the efficiency of atmospheric transport of dust aerosols with diameters above 10 μm over long distances; (iv) pristine conditions are very rarely encountered over the basin.

While much information on the Mediterranean aerosol size distribution has been acquired in recent years, at present, we still miss a complete regional characterization of the aerosol size over the whole basin including seasonal effects. Such regional-scale dataset could be efficiently derived from satellite observations. Many studies reports on data over the Mediterranean from the Moderate Resolution Imaging Spectroradiometer (MODIS) (Papadimas et al., 2008, 2009; Gkikas et al., 2009, 2016), the combination of MODIS and the Total Ozone Mapping Spectrometer (TOMS) (Hatzianastassiou et al., 2009), the Sea-Viewing Wide Field-of-View Sensor (SeaWiFS) (Antoine & Nobileau, 2006), the POLarization and Directionality of the Earth's Reflectances (POLDER) radiometer on PARASOL (Polarization & Anisotropy of Reflectances for Atmospheric Sciences coupled with Observations from a Lidar) (Formenti et al., 2018), or combination of different products (Nabat et al., 2013). Today satellites allow retrieving only partial information, as the column-averaged aerosol Angström exponent or the effective aerosol diameter. Further observation and retrieval capabilities need to be developed in the future to allow retrieving the aerosol size distribution from satellites. This is crucial to improve our understanding of the regional, seasonal, annual, and long-term aerosol size distribution.

Acknowledgments The author wishes to thank P. Formenti for providing a first draft of this section, based on which she developed the full work presented and discussed here.

References

- Alados-Arboledas, L., Müller, D., Guerrero-Rascado, J. L., Navas-Guzmán, F., Pérez-Ramírez, D., & Olmo, F. J. (2011). Optical and microphysical properties of fresh biomass burning aerosol retrieved by Raman lidar, and star-and sun-photometry. *Geophysical Research Letters*, 38, L01807. <https://doi.org/10.1029/2010GL045999>
- Andreae, T. W., Andreae, M. O., Ichoku, C., Maenhaut, W., Cafmeyer, J., Karnieli, A., & Orlovsky, L. (2002). Light scattering by dust and anthropogenic aerosol at a remote site in the Negev desert, Israel. *Journal of Geophysical Research*, 107, 4008. <https://doi.org/10.1029/2001JD900252>
- Angström, A. (1929). On the atmospheric transmission of sun radiation and on dust in the air. *Geografiska Annaler*, 11, 156–166. <https://doi.org/10.1080/20014422.1929.11880498>
- Antoine, D., & Nobileau, D. (2006). Recent increase of Saharan dust transport over the Mediterranean Sea, as revealed from ocean color satellite (SeaWiFS) observations. *Journal of Geophysical Research*, 111, D12214. <https://doi.org/10.1029/2005JD006795>
- Basart, S., Pérez, C., Cuevas, E., Baldasano, J. M., & Gobbi, G. P. (2009). Aerosol characterization in Northern Africa, Northeastern Atlantic, Mediterranean Basin and Middle East from direct-sun AERONET observations. *Atmospheric Chemistry and Physics*, 9, 8265–8282. <https://doi.org/10.5194/acp-9-8265-2009>

- Bauer, S. E., Balkanski, Y., Shulz, M., Hauglustaine, D. A., & Dentener, F. (2004). Global modeling of heterogeneous chemistry on mineral aerosol surfaces: The influence of ozone chemistry and comparison to observations. *Journal of Geophysical Research*, *109*, D02304. <https://doi.org/10.1029/2003JD003868>
- Berland, K., Rose, C., Pey, J., Cuiot, A., Freney, E., Kalivitis, N., Kouvarakis, G., Cerro, J. C., Mallet, M., Sartelet, K., Beckmann, M., Bourriane, T., Roberts, G., Marchand, N., Mihalopoulos, N., & Sellegri, K. (2017). Spatial extent of new particle formation events over the Mediterranean Basin from multiple ground-based and airborne measurements. *Atmospheric Chemistry and Physics*, *17*, 9567–9583. <https://doi.org/10.5194/acp-17-9567-2017>
- Bonasoni, P., Cristofanelli, P., Calzolari, F., Bonafè, U., Evangelisti, F., Stohl, A., Zauli Sajani, S., van Dingenen, R., Colombo, T., & Balkanski, Y. (2004). Aerosol-ozone correlations during dust transport episodes. *Atmospheric Chemistry and Physics*, *4*, 1201–1215. <https://doi.org/10.5194/acp-4-1201-2004>
- Brines, M., Dall'Osto, M., Beddows, D. C. S., Harrison, R. M., & Querol, X. (2014). Simplifying aerosol size distributions modes simultaneously detected at four monitoring sites during SAPUSS. *Atmospheric Chemistry and Physics*, *14*, 2973–2986. <https://doi.org/10.5194/acp-14-2973-2014>
- Chazette, P., & Lioussé, C. (2001). A case study of optical and chemical apportionment for urban aerosols in Thessaloniki. *Atmospheric Environment*, *35*, 2497–2506. [https://doi.org/10.1016/S1352-2310\(00\)00425-8](https://doi.org/10.1016/S1352-2310(00)00425-8)
- Claeys, M., Roberts, G., Mallet, M., Arndt, J., Sellegri, K., Sciare, J., Wenger, J., & Sauvage, B. (2017). Optical, physical and chemical properties of aerosols transported to a coastal site in the western Mediterranean: A focus on primary marine aerosols. *Atmospheric Chemistry and Physics*, *17*, 7891–7915. <https://doi.org/10.5194/acp-17-7891-2017>
- Cusack, M., Pérez, N., Pey, J., Wiedensohler, A., Alastuey, A., & Querol, X. (2013a). Variability of sub-micrometer particle number size distributions and concentrations in the Western Mediterranean regional background. *Tellus*, *65B*, 19243. <https://doi.org/10.3402/tellusb.v65i0.19243>
- Cusack, M., Pérez, N., Pey, J., Alastuey, A., & Querol, X. (2013b). Source apportionment of fine PM and sub-micron particle number concentrations at a regional background site in the western Mediterranean: A 2.5 year study. *Atmospheric Chemistry and Physics*, *13*, 5173–5187. <https://doi.org/10.5194/acp-13-5173-2013>
- Dall'Osto, M., Beddows, D. C. S., Pey, J., Rodriguez, S., Alastuey, A., Harrison, R. M., & Querol, X. (2012). Urban aerosol size distributions over the Mediterranean city of Barcelona, NE Spain. *Atmospheric Chemistry and Physics*, *12*, 10693–10707. <https://doi.org/10.5194/acp-12-10693-2012>
- De Falco, G., Molinaroli, E., & Rabitti, S. (1996). Grain size analysis of aerosol and rain particles: A methodological comparison. In *The impact of desert dust across the Mediterranean, environmental science and technology library* (Vol. 11, pp. 233–238). Springer. https://doi.org/10.1007/978-94-017-3354-0_23
- DeCarlo, P., Slowik, J. G., Worsnop, D. R., Davidovits, P., & Jimenez, J. L. (2004). Particle morphology and density characterization by combined mobility and aerodynamic diameter measurements. Part 1: Theory. *Aerosol Science and Technology*, *38*, 1185–1205. <https://doi.org/10.1080/027868290903907>
- Denjean, C., Cassola, F., Mazzino, A., Triquet, S., Chevaillier, S., Grand, N., Bourriane, T., Momboisse, G., Sellegri, K., Schwarzenbock, A., Freney, E., Mallet, M., & Formenti, P. (2016). Size distribution and optical properties of mineral dust aerosols transported in the western Mediterranean. *Atmospheric Chemistry and Physics*, *16*, 1081–1104. <https://doi.org/10.5194/acp-16-1081-2016>
- Derimian, Y., Karnieli, A., Kaufman, Y. J., Andreae, M. O., Andreae, T. W., Dubovik, O., Maenhaut, W., Koren, I., & Holben, B. N. (2006). Dust and pollution aerosols over the Negev desert, Israel: Properties, transport, and radiative effect. *Journal of Geophysical Research*, *111*, D05205. <https://doi.org/10.1029/2005JD006549>

- Di Biagio, C., Doppler, L., Gaimoz, C., Grand, N., Ancellet, G., Raut, J.-C., Beekmann, M., Borbon, A., Sartelet, K., Attié, J.-L., Ravetta, F., & Formenti, P. (2015). Continental pollution in the western Mediterranean basin: Vertical profiles of aerosol and trace gases measured over the sea during TRAQA 2012 and SAFMED 2013. *Atmospheric Chemistry and Physics*, *15*, 9611–9630. <https://doi.org/10.5194/acp-15-9611-2015>
- Di Biagio, C., Formenti, P., Doppler, L., Gaimoz, C., Grand, N., Ancellet, G., Attié, J.-L., Bucci, S., Dubuisson, P., Fierli, F., Mallet, M., & Ravetta, F. (2016). Continental pollution in the Western Mediterranean basin: Large variability of the aerosol single scattering albedo and influence on the direct shortwave radiative effect. *Atmospheric Chemistry and Physics*, *16*, 10591–10607. <https://doi.org/10.5194/acp-16-10591-2016>
- Di Iorio, T., di Sarra, A., Junkermann, W., Cacciani, M., Fiocco, G., & Fuà, D. (2003). Tropospheric aerosols in the Mediterranean: 1. Microphysical and optical properties. *Journal of Geophysical Research*, *108*, 4316. <https://doi.org/10.1029/2002JD002815>
- di Sarra, A., Anello, F., Bommarito, C., Chamard, P., De Silvestri, L., Di Iorio, T., Fiocco, G., Junkermann, W., Mastrilli, A., Meloni, D., Monteleone, F., Pace, G., Piacentino, S., & Sferlazzo, D. (2005). *The Central-Mediterranean Aerosol and Radiation Experiment (C-MARE): Overview of meteorology and measurements* (Technical Rept. RT-2005-21-CLIM). ENEA.
- Dubovik, O., & King, M. D. (2000). A flexible inversion algorithm for retrieval of aerosol optical properties from sun and sky radiance measurements. *Journal of Geophysical Research*, *105*, 20673–20696. <https://doi.org/10.1029/2000JD900282>
- Dubovik, O., Sinyuk, A., Lapyonok, T., Holben, B. N., Mishchenko, M., Yang, P., Eck, T. F., Volten, H., Muñoz, O., Veihelmann, B., van der Zande, W. J., Leon, J.-F., Sorokin, M., & Slutsker, I. (2006). Application of spheroid models to account for aerosol particle non sphericity in remote sensing of desert dust. *Journal of Geophysical Research*, *111*, D11208. <https://doi.org/10.1029/2005JD006619>
- Dulac, F., & Chazette, P. (2003). Airborne study of a multi-layer aerosol structure in the eastern Mediterranean observed with the airborne polarized lidar ALEX during a STAAARTE campaign (7 June 1997). *Atmospheric Chemistry and Physics*, *3*, 1817–1831. <https://doi.org/10.5194/acp-3-1817-2003>
- Dulac, F., Buat-Ménard, P., Ezat, U., Melki, S., & Bergametti, G. (1989). Atmospheric input of trace metals to the western Mediterranean: Uncertainties in modelling dry deposition from cascade impactor data. *Tellus*, *41B*, 362–378. <https://doi.org/10.1111/j.1600-0889.1989.tb00315.x>
- Dulac, F., Sauvage, S., Hamonou, E., & Debevec, C. (2023). Introduction to the volume 1 of Atmospheric Chemistry in the Mediterranean Region and to the experimental effort during the ChArMEx decade. In F. Dulac, S. Sauvage, & E. Hamonou (Eds.), *Atmospheric chemistry in the Mediterranean Region* (Vol. 1, Background information and pollutant distribution). Springer.
- Foret, G., Bergametti, G., Dulac, F., & Menut, L. (2006). An optimized particle size bin scheme for modeling mineral dust aerosol. *Journal of Geophysical Research*, *111*, D17310. <https://doi.org/10.1029/2005JD006797>
- Formenti, P., Andreae, M. O., Ichoku, C., Andreae, T. W., Schebeske, G., Kettle, A. J., Maenhaut, W., Cafmeyer, J., Ptasinaky, J., Karnieli, A., & Lelieveld, J. (2001). Physical and chemical characteristics of aerosols over the Negev desert (Israel) during summer 1996. *Journal of Geophysical Research*, *106*, 4871–4890. <https://doi.org/10.1029/2000JD900556>
- Formenti, P., Reiner, T., Sprung, D., Andreae, M. O., Wendisch, M., Wex, H., Kindred, D., Dewey, K., Kent, J., Tzortziou, M., Vasaras, A., & Zerefos, C. (2002). STAAARTE-MED 1998 summer airborne measurements over the Aegean Sea: 1. Aerosol particles and trace gases. *Journal of Geophysical Research*, *107*, 4450. <https://doi.org/10.1029/2001JD001337>
- Formenti, P., Schütz, L., Balkanski, Y., Desboeufs, K., Ebert, M., Kandler, K., Petzold, A., Scheuvs, D., Weinbruch, S., & Zhang, D. (2011). Recent progress in understanding physical and chemical properties of African and Asian mineral dust. *Atmospheric Chemistry and Physics*, *11*, 8231–8256. <https://doi.org/10.5194/acp-11-8231-2011>

- Formenti, P., Mbemba Kabuiku, L., Chiapello, I., Ducos, F., Dulac, F., & Tanré, D. (2018). Aerosol optical properties derived from POLDER-3/PARASOL (2005–2013) over the western Mediterranean Sea – Part 1: Quality assessment with AERONET and in situ airborne observations. *Atmospheric Measurement Techniques*, *11*, 6761–6784. <https://doi.org/10.5194/amt-11-6761-2018>
- Fotiadi, A., Hatzianastassiou, N., Drakakis, E., Matsoukas, C., Pavlakis, K. G., Hatzidimitriou, D., Gerasopoulos, E., Mihalopoulos, N., & Vardavas, I. (2006). Aerosol physical and optical properties in the Eastern Mediterranean Basin, Crete, from Aerosol Robotic Network data. *Atmospheric Chemistry and Physics*, *6*, 5399–5413. <https://doi.org/10.5194/acp-6-5399-2006>
- Gerasopoulos, E., Koulouri, E., Kalivitis, N., Kouvarakis, G., Saarikoski, S., Mäkelä, T., Hillamo, R., & Mihalopoulos, N. (2007). Size-segregated mass distributions of aerosols over Eastern Mediterranean: Seasonal variability and comparison with AERONET columnar size-distributions. *Atmospheric Chemistry and Physics*, *7*, 2551–2561. <https://doi.org/10.5194/acp-7-2551-2007>
- Gkikas, A., Hatzianastassiou, N., & Mihalopoulos, N. (2009). Aerosol events in the broader Mediterranean basin based on 7-year (2000–2007) MODIS C005 data. *Annales de Geophysique*, *27*, 3509–3522. <https://doi.org/10.5194/angeo-27-3509-2009>
- Gkikas, A., Basart, S., Hatzianastassiou, N., Marinou, E., Amiridis, V., Kazadzis, S., Pey, J., Querol, X., Jorba, O., Gassó, S., & Baldasano, J. M. (2016). Mediterranean intense desert dust outbreaks and their vertical structure based on remote sensing data. *Atmospheric Chemistry and Physics*, *16*, 8609–8642. <https://doi.org/10.5194/acp-16-8609-2016>
- Gómez-Amo, J. L., Estellés, V., Marcos, C., Segura, S., Esteve, A. R., Pedrós, R., Utrillas, M. P., & Martínez-Lozano, J. A. (2017). Impact of dust and smoke mixing on column-integrated aerosol properties from observations during a severe wildfire episode over Valencia (Spain). *The Science of the Total Environment*, *599–600*, 2121–2134. <https://doi.org/10.1016/j.scitotenv.2017.05.041>
- Hamburger, T., McMeeking, G., Minikin, A., Petzold, A., Coe, H., & Krejci, R. (2012). Airborne observations of aerosol microphysical properties and particle ageing processes in the troposphere above Europe. *Atmospheric Chemistry and Physics*, *12*, 11533–11554. <https://doi.org/10.5194/acp-12-11533-2012>
- Hatzianastassiou, N., Gkikas, A., Mihalopoulos, N., Torres, O., & Katsoulis, B. D. (2009). Natural versus anthropogenic aerosols in the eastern Mediterranean basin derived from multiyear TOMS and MODIS satellite data. *Journal of Geophysical Research*, *114*, D24202. <https://doi.org/10.1029/2009JD011982>
- Highwood, E. J., Northway, M. J., McMeeking, G. R., Morgan, W. T., Liu, D., Osborne, S., Bower, K., Coe, H., Ryder, C., & Williams, P. (2012). Aerosol scattering and absorption during the EUCAARI-LONGREX flights of the Facility for Airborne Atmospheric Measurements (FAAM) BAe-146: Can measurements and models agree? *Atmospheric Chemistry and Physics*, *12*, 7251–7267. <https://doi.org/10.5194/acp-12-7251-2012>
- Holben, B. N., Eck, T. F., Slutsker, I., Tanré, D., Buis, J. P., Setzer, A., Vermote, E., Reagan, J. A., Kaufman, Y. J., Nakajima, T., Lavenu, F., Jankowiak, I., & Smirnov, A. (1998). AERONET – A federated instrument network and data archive for aerosol characterization. *Remote Sensing of Environment*, *66*, 1–16. [https://doi.org/10.1016/S0034-4257\(98\)00031-5](https://doi.org/10.1016/S0034-4257(98)00031-5)
- Ichoku, C., Andreae, M. O., Andreae, T. W., Meixner, F. X., Shebeske, G., & Formenti, P. (1999). Interrelationships between aerosol characteristics and light scattering during late winter in an eastern Mediterranean arid environment. *Journal of Geophysical Research*, *104*, 24371–24393. <https://doi.org/10.1029/1999JD900781>
- Jaenicke, R. (1988). Aerosol physics and chemistry. In *Landolt-Börnstein numerical data and functional relationships in science and technology*, *4b* (pp. 391–457). Springer.
- Junkermann, W. (2001). An ultralight aircraft as platform for research in the lower troposphere: System performance and first results from radiation transfer studies in stratiform aerosol layers and broken cloud conditions. *Journal of Atmospheric and Oceanic Technology*, *18*, 934–946. [https://doi.org/10.1175/1520-0426\(2001\)018<0934:AUAAPP>2.0.CO;2](https://doi.org/10.1175/1520-0426(2001)018<0934:AUAAPP>2.0.CO;2)

- Junkermann, W. (2009). On the distribution of formaldehyde in the western Po-Valley, Italy, during 2002/2003. *Atmospheric Chemistry and Physics*, 9, 9187–9196. <https://doi.org/10.5194/acp-9-9187-2009>
- Junkermann, W. (2022). Ultrafine particle emissions in the Mediterranean. In F. Dulac, S. Sauvage, & E. Hamonou (Eds.), *Atmospheric chemistry in the Mediterranean Region* (Vol. 2, From air pollutant sources to impacts). Springer, this volume. https://doi.org/10.1007/978-3-030-82385-6_6
- Kalivitis, N., Kerminen, V.-M., Kouvarakis, G., Stavroulas, I., Tzitzikalaki, E., Kalkavouras, P., Daskalakis, N., Myriokefalitakis, S., Bougiatioti, A., Manninen, H. E., Roldin, P., Petäjä, T., Boy, M., Kulmala, M., Kanakidou, M., & Mihalopoulos, N. (2019). Formation and growth of atmospheric nanoparticles in the eastern Mediterranean: Results from long-term measurements and process simulations. *Atmospheric Chemistry and Physics*, 19, 2671–2686. <https://doi.org/10.5194/acp-19-2671-2019>
- Koehler, K. A., Kreidenweis, S. M., DeMott, P. J., Petters, M. D., Prenni, A. J., & Carrico, C. M. (2009). Hygroscopicity and cloud droplet activation of mineral dust aerosol. *Geophysical Research Letters*, 36, L08805. <https://doi.org/10.1029/2009GL037348>
- Kopanakis, I., Chatoutsidou, S. E., Torseth, K., Glytsos, T., & Lazaridis, M. (2013). Particle number size distribution in the eastern Mediterranean: Formation and growth rates of ultrafine airborne atmospheric particles. *Atmospheric Environment*, 77, 790–802. <https://doi.org/10.1016/j.atmosenv.2013.05.066>
- Kubilay, N., Cokacar, T., & Oguz, T. (2003). Optical properties of mineral dust outbreaks over the northeastern Mediterranean. *Journal of Geophysical Research*, 108, 4666. <https://doi.org/10.1029/2003JD003798>
- Kuloglu, E., & Tuncel, G. (2005). Size distribution of trace elements and major ions in the eastern Mediterranean atmosphere. *Water, Air, and Soil Pollution*, 167, 221–241. <https://doi.org/10.1007/s11270-005-8651-3>
- Logothetis, S. A., Salamalikis, V., & Kazantzidis, A. (2020). Aerosol classification in Europe, Middle East, North Africa and Arabian Peninsula based on AERONET version 3. *Atmospheric Research*, 239, 15, 104893. <https://doi.org/10.1016/j.atmosres.2020.104893>
- Maenhaut, W., Ptasinaki, J., & Cafmeyer, J. (1999). Detailed mass size distributions of atmospheric aerosol species in the Negev desert, Israel, during ARACHNE-96. *Nuclear Instruments and Methods in Physics Research Section B*, 150, 422–427. [https://doi.org/10.1016/S0168-583X\(98\)01069-6](https://doi.org/10.1016/S0168-583X(98)01069-6)
- Mallet, M., Roger, J. C., Despiiau, S., Dubovik, O., & Putaud, J. P. (2003). Microphysical and optical properties of aerosol particles in urban zone during ESCOMPTE. *Atmospheric Research*, 69, 73–97. <https://doi.org/10.1016/j.atmosres.2003.07.001>
- Mallet, M., Van Dingenen, R., Roger, J. C., Despiiau, S., & Cachier, H. (2005). In situ airborne measurements of aerosol optical properties during photochemical pollution events. *Journal of Geophysical Research*, 110, D03205. <https://doi.org/10.1029/2004JD005139>
- Mallet, M., Dubovik, O., Nabat, P., Dulac, F., Kahn, R., Sciare, J., Paronis, D., & Léon, J. F. (2013). Absorption properties of Mediterranean aerosols obtained from multi-year ground-based remote sensing observations. *Atmospheric Chemistry and Physics*, 13, 9195–9210. <https://doi.org/10.5194/acp-13-9195-2013>
- Mallet, M., Dulac, F., Formenti, P., Nabat, P., Sciare, J., Roberts, G., Pelon, J., Ancellet, G., Tanré, D., Parol, F., Denjean, C., Brogniez, G., di Sarra, A., Alados-Arboledas, L., Arndt, J., Auriol, F., Blarel, L., Bourriane, T., Chazette, P., ... Zapf, P. (2016). Overview of the Chemistry-Aerosol Mediterranean Experiment/Aerosol Direct Radiative Forcing on the Mediterranean Climate (ChArMEx/ADRIMED) summer 2013 campaign. *Atmospheric Chemistry and Physics*, 16, 455–504. <https://doi.org/10.5194/acp-16-455-2016>
- Mallet, M. D., D'Anna, B., Mème, A., Bove, M. C., Cassola, F., Pace, G., Desboeufs, K., Di Biagio, C., Doussin, J.-F., Maille, M., Massabò, D., Sciare, J., Zapf, P., di Sarra, A. G., & Formenti, P. (2019). Summertime surface PM₁ aerosol composition and size by source region at the Lampedusa island in the central Mediterranean Sea. *Atmospheric Chemistry and Physics*, 19, 11123–11142. <https://doi.org/10.5194/acp-19-11123-2019>

- Masmoudi, M., Chaabane, M., Tanré, D., Gouloup, P., Blarel, L., & Elleuch, F. (2003a). Spatial and temporal variability of aerosol: Size distribution and optical properties. *Atmospheric Research*, *66*, 1–19. [https://doi.org/10.1016/S0169-8095\(02\)00174-6](https://doi.org/10.1016/S0169-8095(02)00174-6)
- Masmoudi, M., Chaabane, M., Medhioub, K., & Euch, F. (2003b). Variability of aerosol optical thickness and atmospheric turbidity in Tunisia. *Atmospheric Research*, *66*, 175–188. [https://doi.org/10.1016/S0169-8095\(02\)00175-8](https://doi.org/10.1016/S0169-8095(02)00175-8)
- Meloni, D., Junkermann, W., di Sarra, A., Cacciani, M., De Silvestri, L., Di Iorio, T., Estellés, V., Gómez-Amo, J. L., Pace, G., & Sferlazzo, D. M. (2015). Altitude-resolved shortwave and long-wave radiative effects 1 of desert dust in the Mediterranean during the GAMARF campaign: Indications of a net daily cooling in the dust layer. *Journal of Geophysical Research*, *120*, 3386–3407. <https://doi.org/10.1002/2014JD022312>
- Mishchenko, M. I., Travis, L. D., Kahn, R. A., & West, R. A. (1997). Modeling phase function for dustlike tropospheric aerosols using a shape mixture of randomly oriented poly-disperse spheroids. *Journal of Geophysical Research*, *102*, 16831–16847. <https://doi.org/10.1029/96JD02110>
- Nabat, P., Somot, S., Mallet, M., Chiapello, I., Morcrette, J. J., Solmon, F., Szopa, S., Dulac, F., Collins, W., Ghan, S., Horowitz, L. W., Lamarque, J. F., Lee, Y. H., Naik, V., Nagashima, T., Shindell, D., & Skeie, R. (2013). A 4-D climatology (1979–2009) of the monthly tropospheric aerosol optical depth distribution over the Mediterranean region from a comparative evaluation and blending of remote sensing and model products. *Atmospheric Measurement Techniques*, *6*, 1287–1314. <https://doi.org/10.5194/amt-6-1287-2013>
- Pace, G., di Sarra, A., Meloni, D., Piacentino, S., & Chamard, P. (2006). Aerosol optical properties at Lampedusa (Central Mediterranean). 1. Influence of transport and identification of different aerosol types. *Atmospheric Chemistry and Physics*, *6*, 697–713. <https://doi.org/10.5194/acp-6-697-2006>
- Pace, G., Junkermann, W., Vitali, L., di Sarra, A., Meloni, D., Cacciani, M., Cremona, G., Iannarelli, A. M., & Zanini, G. (2015). On the complexity of the boundary layer structure and aerosol vertical distribution in the coastal Mediterranean regions: A case study. *Tellus B: Chemical and Physical Meteorology*, *67*, 27721. <https://doi.org/10.3402/tellusb.v67.27721>
- Papadimas, C. D., Hatzianastassiou, N., Mihalopoulos, N., Querol, X., & Vardavas, I. (2008). Spatial and temporal variability in aerosol properties over the Mediterranean basin based on 6-year (2000–2006) MODIS data. *Journal of Geophysical Research*, *113*, D11205. <https://doi.org/10.1029/2007JD009189>
- Papadimas, C. D., Hatzianastassiou, N., Mihalopoulos, N., Kanakidou, M., Katsoulis, B. D., & Vardavas, I. (2009). Assessment of the MODIS collections C005 and C004 aerosol optical depth products over the Mediterranean basin. *Atmospheric Chemistry and Physics*, *9*, 2987–2999. <https://doi.org/10.5194/acp-9-2987-2009>
- Petzold, A., Fiebig, M., Flentje, H., Keil, A., Leiterer, U., Schroder, F., Stifter, A., Wendisch, M., & Wendling, P. (2002). Vertical variability of aerosol properties observed at a continental site during the Lindenberg Aerosol Characterization Experiment (LACE 98). *Journal of Geophysical Research*, *107*, 8128. <https://doi.org/10.1029/2001JD001043>
- Pey, J., Rodríguez, S., Querol, X., Alastuey, A., Moreno, T., Putaud, J. P., & Van Dingenen, R. (2008). Variations of urban aerosols in the western Mediterranean. *Atmospheric Environment*, *42*, 9052–9062. <https://doi.org/10.1016/j.atmosenv.2008.09.049>
- Pey, J., Querol, X., Alastuey, A., Rodríguez, S., Putaud, J. P., & Van Dingenen, R. (2009). Source apportionment of urban fine and ultra fine particle number concentration in a Western Mediterranean city. *Atmospheric Environment*, *43*, 4407–4415. <https://doi.org/10.1016/j.atmosenv.2009.05.024>
- Renard, J.-B., Dulac, F., Berthet, G., Lurton, T., Vignelles, D., Jégou, F., Tonnelier, T., Jeannot, M., Couté, B., Akiki, R., Verdier, N., Mallet, M., Gensdarmes, F., Charpentier, P., Mesmin, S., Duverger, V., Dupont, J.-C., Elias, T., Crenn, V., ... Daugeron, D. (2016). LOAC: A small aerosol optical counter/sizer for ground-based and balloon measurements of the size distribution and nature of atmospheric particles – Part 2: First results from balloon and unmanned aerial

- vehicle flights. *Atmospheric Measurement Techniques*, 9, 3673–3686. <https://doi.org/10.5194/amt-9-3673-2016>
- Renard, J.-B., Dulac, F., Durand, P., Bourgeois, Q., Denjean, C., Vignelles, D., Couté, B., Jeannot, M., Verdier, N., & Mallet, M. (2018). In situ measurements of desert dust particles above the western Mediterranean Sea with the balloon-borne Light Optical Aerosol Counter/sizer (LOAC) during the ChArMEX campaign of summer 2013. *Atmospheric Chemistry and Physics*, 18, 3677–3699. <https://doi.org/10.5194/acp-18-3677-2018>
- Rose, C., Sellegri, K., Freney, E., Dupuy, R., Colomb, A., Pichon, J.-M., Ribeiro, M., Bourianne, T., Burnet, F., & Schwarzenboeck, A. (2015). Airborne measurements of new particle formation in the free troposphere above the Mediterranean Sea during the HYMEX campaign. *Atmospheric Chemistry and Physics*, 15, 10203–10218. <https://doi.org/10.5194/acp-15-10203-2015>
- Ryder, C. L., Highwood, E. J., Lai, T. M., Sodemann, H., & Marsham, J. H. (2013). Impact of atmospheric transport on the evolution of microphysical and optical properties of Saharan dust. *Geophysical Research Letters*, 40, 2433–2438. <https://doi.org/10.1002/grl.50482>
- Ryder, C. L., Marengo, F., Brooke, J. K., Estelles, V., Cotton, R., Formenti, P., McQuaid, J. B., Price, H. C., Liu, D., Ausset, P., Rosenberg, P. D., Taylor, J. W., Choularton, T., Bower, K., Coe, H., Gallagher, M., Crosier, J., Lloyd, G., Highwood, E. J., & Murray, B. J. (2018). Coarse-mode mineral dust size distributions, composition and optical properties from AER-D aircraft measurements over the tropical eastern Atlantic. *Atmospheric Chemistry and Physics*, 18, 17225–17257. <https://doi.org/10.5194/acp-18-17225-2018>
- Sabbah, I., Ichoku, C., Kaufman, Y. J., & Remer, L. (2001). Full year cycle of desert dust spectral optical thickness and precipitable water vapor over Alexandria, Egypt. *Journal of Geophysical Research*, 106, 18305–18316. <https://doi.org/10.1029/2000JD900410>
- Sayer, A. M., Hsu, N. C., Eck, T. F., Smirnov, A., & Holben, B. N. (2014). AERONET-based models of smoke-dominated aerosol near source regions and transported over oceans, and implications for satellite retrievals of aerosol optical depth. *Atmospheric Chemistry and Physics*, 14, 11493–11523. <https://doi.org/10.5194/acp-14-11493-2014>
- Seinfeld, J. H., & Pandis, S. N. (2016). *Atmospheric chemistry and physics: From air pollution to climate change* (3rd ed.). Wiley, 1152 pp.
- Sicard, M., Barragan, R., Dulac, F., Alados-Arboledas, L., & Mallet, M. (2016). Aerosol optical, microphysical and radiative properties at regional background insular sites in the western Mediterranean. *Atmospheric Chemistry and Physics*, 16, 12177–12203. <https://doi.org/10.5194/acp-16-12177-2016>
- Sanchez-Marroquin, A., Hedges, D. H. P., Hiscock, M., Parker, S. T., Rosenberg, P. D., Trembath, J., Walshaw, R., Burke, I. T., McQuaid, J. B., & Murray, B. J. (2019). Characterisation of the filter inlet system on the FAAM BAe-146 research aircraft and its use for size-resolved aerosol composition measurements. *Atmospheric Measurements Techniques*, 12, 5741–5763. <https://doi.org/10.5194/amt-12-5741-2019>, 2019
- Smolík, J., Ždímal, V., Schwarz, J., Lazaridis, M., Havárnek, V., Eleftheriadis, K., Mihalopoulos, N., Bryant, C., & Colbeck, I. (2003). Size resolved mass concentration and elemental composition of atmospheric aerosols over the Eastern Mediterranean area, *Atmos. Chem. Phys.*, 3, 2207–2216. <https://doi.org/10.5194/acp-3-2207-20033/>
- Tafuro, A. M., Banaba, F., De Tomasi, F., Perrone, M. R., & Gobbi, G. P. (2006). Saharan dust particle properties over the central Mediterranean. *Atmospheric Research*, 81, 67–93. <https://doi.org/10.1016/j.atmosres.2005.11.008>
- Toledano, C., Cachorro, V. E., Berjon, A., de Frutos, A. M., Sorribas, M., de la Morena, B. A., & Goloub, P. (2007). Aerosol optical depth and Ångström exponent climatology at El Arenosillo AERONET site (Huelva, Spain). *Quarterly Journal of the Royal Meteorological Society*, 133, 795–807. <https://doi.org/10.1002/qj.54>
- van der Does, M., Knippertz, P., Zschenderlein, P., Harrison, R. G., & Stuut, J.-B. W. (2018). The mysterious long-range transport of giant mineral dust particles. *Science Advances*, 4, eaau2768. <https://doi.org/10.1126/sciadv.aau2768>

- Van Dingenen, R., Putaud, J.-P., Martins-Dos Santos, S., & Raes, F. (2005). Physical aerosol properties and their relation to air mass origin at Monte Cimone (Italy) during the first MINATROC campaign. *Atmospheric Chemistry and Physics*, 5, 2203–2226. <https://doi.org/10.5194/acp-5-2203-2005>
- Weinzierl, B., Sauer, D., Esselborn, M. M., Petzold, A., Veira, A., Rose, M., Mund, S., Wirth, M., Ansmann, A., Tesche, M., Gross, S., & Freudenthaler, V. (2011). Microphysical and optical properties of dust and tropical biomass burning aerosol layers in the Cape Verde region—an overview of the airborne in situ and lidar measurements during SAMUM-2. *Tellus B: Chemical and Physical Meteorology*, 63, 589–618. <https://doi.org/10.1111/j.1600-0889.2011.00566.x>
- Weinzierl, B., Ansmann, A., Prospero, J. M., Althausen, D., Benker, N., Chouza, F., Dollner, M., Farrell, D., Fomba, W. K., Freudenthaler, V., Gasteiger, J., Groß, S., Haarig, M., Heinold, B., Kandler, K., Kristensen, T. B., Mayol-Bracero, O. L., Müller, T., Reitebuch, O., ... Walser, A. (2017). The Saharan aerosol long-range transport and aerosol–cloud–interaction experiment: Overview and selected highlights. *Bulletin of the American Meteorological Society*, 98, 1427–1451. <https://doi.org/10.1175/BAMS-D-15-00142.1>
- Wiegner, M., Emeis, S., Freudenthaler, V., Heese, B., Junkermann, W., Munkel, C., Schäfer, K., Seefeldner, M., & Vogt, S. (2006). Mixing layer height over Munich, Germany: Variability and comparisons of different methodologies. *Journal of Geophysical Research*, 111, D13201. <https://doi.org/10.1029/2005JD006593>